

Nickel Complexes with Phosphinito-Oxazoline Ligands: Temperature-Controlled Formation of Mono- or Dinuclear Complexes and Catalytic Oligomerization of Ethylene and Propylene

Patricia Chavez,[†] Itzel Guerrero Rios,[‡] Anthony Kermagoret,[†] Roberto Pattacini,[†] Andrea Meli,[‡] Claudio Bianchini,[‡] Giuliano Giambastiani,^{*,‡} and Pierre Braunstein^{*,†}

Laboratoire de Chimie de Coordination, Institut de Chimie (UMR 7177 CNRS), Université de Strasbourg, 4 rue Blaise Pascal, F-67070 Strasbourg Cédex, France, and Institute of Chemistry of Organometallic Compounds, ICCOM-CNR, Via Madonna del Piano, 10 - 50019 Sesto Fiorentino (Fi), Italy

Received October 12, 2008

The complex $[\text{NiCl}_2\{\text{Ph}_2\text{POCH}_2\text{ox}^{\text{Me}_2}\}]$ ($\text{Ph}_2\text{POCH}_2\text{ox}^{\text{Me}_2} = 2\text{-}((\text{diphenylphosphinoxy})\text{methyl})\text{-}4,4\text{-dimethyl-}4,5\text{-dihydrooxazole}$) **14** has been synthesized by reaction of solid $[\text{NiCl}_2(\text{DME})]$ (DME = 1,2-dimethoxyethane) with a CH_2Cl_2 solution of the P,N ligand. X-ray diffraction studies on its red crystals established the mononuclear nature of the complex **14a**, whose metal center has a distorted tetrahedral coordination geometry. Recrystallization of **14a** from a toluene–pentane/ CH_2Cl_2 solution at temperatures below 253 K afforded green crystals of the dinuclear, chloride-bridged, formula isomer complex **14b**. Conversion of **14b** to **14a** was observed as a function of temperature, both in the solid-state and in solution. Together with other Ni(II) complexes containing a chelating P,N ligand of the type phosphino- or phosphinito-oxazoline or phosphino-thiazoline, **14a** has been evaluated as precatalyst in the oligomerization of ethylene, with AlEtCl_2 or MAO as cocatalyst, or propylene, with MAO as cocatalyst. With AlEtCl_2 as activator (6 equiv), the catalytic activities with ethylene were generally modest and $[\text{NiCl}_2\{\text{Ph}_2\text{PCH}_2\text{ox}\}]$ ($\text{Ph}_2\text{PCH}_2\text{ox} = 2\text{-}((\text{diphenylphosphinoxy})\text{methyl})\text{-}4,5\text{-dihydrooxazole}$) **1** was the most active, with turnover frequencies (TOF) up to 7.9×10^4 mol of C_2H_4 (mol Ni \times h)⁻¹, whereas **14a**, activated with 2 equiv of AlEtCl_2 , was the most selective for ethylene dimers (up to 96%) and 1-butene (up to 22%). With MAO as cocatalyst, complex **1** was again the most active, with TOF values up to 23×10^4 mol of C_2H_4 (mol Ni \times h)⁻¹. The highest selectivity for butenes was observed with complex $[\text{NiCl}_2\{\text{Ph}_2\text{PCH}_2\text{thiaz}^{\text{Me}_2}\}]$ **3**. With propylene, TOFs up to 3.3×10^4 mol of C_3H_6 (mol Ni \times h)⁻¹ were obtained with $[\text{NiCl}_2\{\text{Ph}_2\text{POCH}_2\text{pyridine}\}]$ **8** and selectivities for C_6 products higher than 98.5% were observed with precatalysts **3**, $[\text{NiCl}_2\{t\text{-Bu}_2\text{POCH}_2\text{pyridine}\}]$ **9**, and **14a**.

Introduction

Heterofunctional ligands are much studied and applied in coordination and organometallic chemistry owing to the often unique properties of their metal complexes and their ability to generate hemilabile systems endowed with enhanced reactivity.¹ The combination of a hard nitrogen donor with a soft phosphorus donor within a functional ligand leads to considerable chemical and structural diversity and the resulting metal complexes often display important applications in homogeneous catalysis, in particular because of the stereoelectronic differentiation brought about by the different donor functions and the stabilization of the metal ion in optimum oxidation states.^{1–3} Chelating P,N ligands containing N-heterocycles, such as pyridyl- and oxazolyl-, have been much investigated and their nickel complexes are active catalyst precursors in the catalytic oligomerization

of ethylene,^{3–5} a reaction of major industrial interest.⁶ Indeed, since the seminal works of Ziegler and Natta on the oligomerization and polymerization of ethylene with metal catalysts activated by alkyl aluminums,⁷ major industrial developments

* To whom correspondence should be addressed. E-mail: braunstein@chimie.u-strasbg.fr, giuliano.giambastiani@iccom.cnr.it.

[†] Université de Strasbourg, France.

[‡] ICCOM-CNR, Sesto Fiorentino, Italy.

(1) (a) Bader, A.; Lindner, E. *Coord. Chem. Rev.* **1991**, *108*, 27. (b) Slone, C. S.; Weinberger, D. A.; Mirkin, C. A. *Prog. Inorg. Chem.* **1999**, *48*, 233. (c) Helmchen, G.; Pfaltz, A. *Acc. Chem. Res.* **2000**, *33*, 336. (d) Braunstein, P.; Naud, F. *Angew. Chem., Int. Ed.* **2001**, *40*, 680. (e) McManus, H. A.; Guiry, P. J. *Chem. Rev.* **2004**, *104*, 4151. (f) Margraf, G.; Pattacini, R.; Messaoudi, A.; Braunstein, P. *Chem. Commun.* **2006**, 3098. (g) Braunstein, P. *Chem. Rev.* **2006**, *106*, 134.

(2) (a) Bianchini, C.; Meli, A.; Peruzzini, M.; Vizza, F.; Zanobini, F. *Coord. Chem. Rev.* **1992**, *120*, 193. (b) Newkome, G. R. *Chem. Rev.* **1993**, *93*, 2067. (c) Ajjou, A. N.; Alper, H. *J. Am. Chem. Soc.* **1998**, *120*, 1466. (d) Espinet, P.; Soulantica, K. *Coord. Chem. Rev.* **1999**, 193–195. (e) Qadir, M.; Mochel, T.; Hii, K. K. *Tetrahedron* **2000**, *56*, 7975. (f) Hierso, J.-C.; Amardeil, R.; Bentabet, E.; Broussier, R.; Gautheron, B.; Meunier, P.; Kalck, P. *Coord. Chem. Rev.* **2003**, *236*, 143.

(3) Speiser, F.; Braunstein, P.; Saussine, L. *Acc. Chem. Res.* **2005**, *38*, 784.

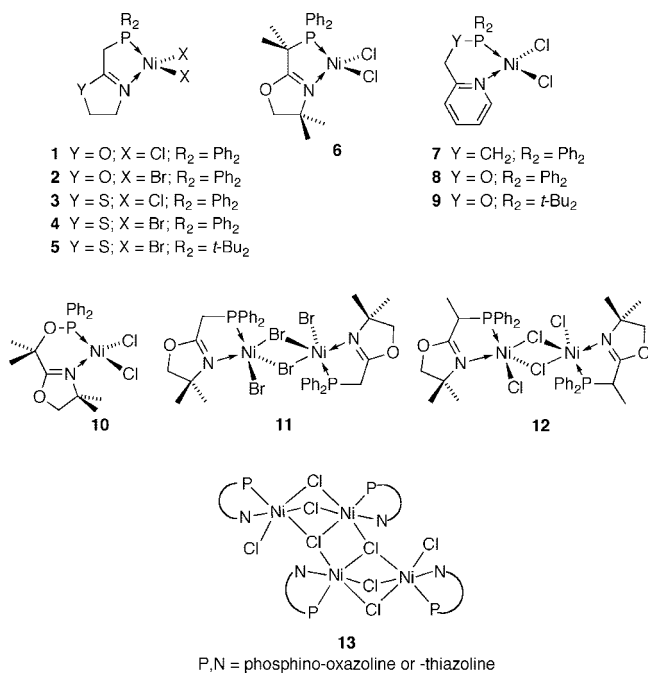
(4) (a) Bluhm, M. E.; Folli, C.; Walter, O.; Doering, M. *J. Mol. Catal. A, Chem.* **2005**, *229*, 177. (b) Mukherjee, A.; Subramanyam, U.; Puranik, V. G.; Mohandas, T. P.; Sarkar, A. *Eur. J. Inorg. Chem.* **2005**, 1254. (c) Sirbu, D.; Consiglio, G.; Gischig, S. *J. Organomet. Chem.* **2006**, *691*, 1143. (d) Speiser, F.; Braunstein, P.; Saussine, L. *Organometallics* **2004**, *23*, 2625. (e) Speiser, F.; Braunstein, P.; Saussine, L. *Organometallics* **2004**, *23*, 2633. (f) Sun, W.-H.; Li, Z.; Hu, H.; Wu, B.; Yang, H.; Zhu, N.; Leng, X.; Wang, H. *New J. Chem.* **2002**, *26*, 1474. (g) Tang, X.; Zhang, D.; Jie, S.; Sun, W.-H.; Chen, J. *J. Organomet. Chem.* **2005**, *690*, 3918.

(5) Kermagoret, A.; Braunstein, P. *Organometallics* **2008**, *27*, 88.

(6) Vogt, D., Ed. *Applied Homogeneous Catalysis with Organometallic Compounds*; VCH: Weinheim, 2002. (b) Gibson, V. C.; Spitzmesser, S. K. *Chem. Rev.* **2003**, *103*, 283. (c) Ittel, S. D.; Johnson, L. K.; Brookhart, M. *Chem. Rev.* **2000**, *100*, 1169.

(7) (a) Ziegler, K.; Holzkamp, E.; Breil, H.; Martin, H. *Angew. Chem.* **1955**, *67*, 426. (b) Wilke, G. *Angew. Chem., Int. Ed.* **2003**, *42*, 5000. (c) Bolton, P. D.; Mountford, P. *Adv. Synth. Catal.* **2005**, *347*, 355. (d) Böhm, L. L. *Angew. Chem., Int. Ed.* **2003**, *42*, 5010.

Scheme 1



in the catalytic production of linear α -olefins (LAO) have taken place. Complexes of the late transition metals such as Ni, Pd, Co, and Fe give rise to oligomerization precatalysts by favoring chain transfer over propagation during the catalytic cycle.^{3,8}

Some of us have recently prepared a range of Ni(II) complexes with a P,N chelating ligand containing a phosphine or a phosphite donor associated with an oxazoline or a thiazoline heterocycle and studied the catalytic properties of some of them in ethylene oligomerization as a function of the chelate ring size, the nature of the phosphorus function, the cocatalyst (MAO or AlEtCl₂) and in some cases compared them with their analogues containing a pyridine donor in place of the oxazoline (see **1–12**, Scheme 1).^{3,5} The nuclearity of the complexes and the coordination geometry around the Ni center(s) (square-planar, tetrahedral, trigonal bipyramidal, with varying degrees of distortion) were found to be very sensitive to the chelate ring size and its substitution pattern.

It was also found that unprecedented tetranuclear complexes of the type $[\{Ni_2(\mu_2-Cl)_2Cl(P,N)_2\}_2(\mu_3-Cl)_2]$ (**13**) could form and undergo in the solid-state an irreversible pressure-induced fragmentation into the corresponding mononuclear complex $[NiCl_2(P,N)]$ (**1** or **3**).⁹ These observations triggered our interest for further studies, reported below, on these classes of compounds and their catalytic properties in ethylene and propylene oligomerization.

Results

Synthesis and X-Ray Crystal Structures of 14a and 14b and Their Interconversion. The complex $[NiCl_2\{Ph_2POCH_2ox^{Me_2}\}]$ ($Ph_2POCH_2ox^{Me_2} = 2-((diphenylphosphinooxy)methyl)-4,4-$ di-

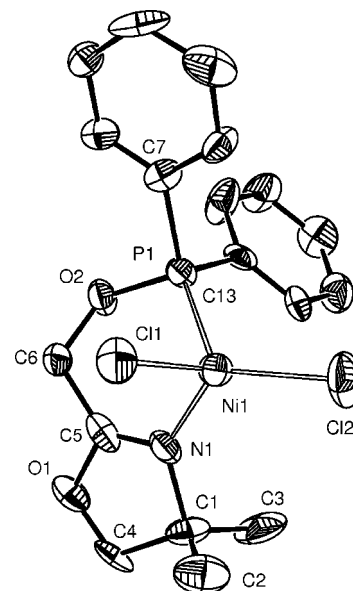
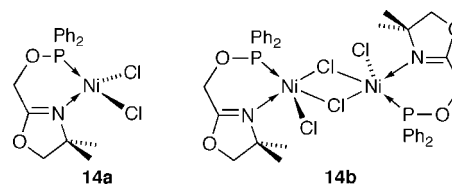


Figure 1. ORTEP plot of the molecular structure of **14a**. Hydrogen atoms have been omitted for clarity. Selected distances (Å) and angles (°): Ni1–N1 1.977(7), Ni1–Cl1 2.234(2), Ni1–Cl2 2.179(3), Ni1–P1 2.264(2), N1–C5 1.25(1); N1–Ni1–Cl1 98.3(2), N1–Ni1–Cl2 118.1(2), Cl1–Ni1–Cl2 127.5(1), N1–Ni1–P1 90.5(2), Cl1–Ni1–P1 101.2(1), Cl2–Ni1–P1 113.9(1).

methyl-4,5-dihydrooxazole) **14** was synthesized by reacting $[NiCl_2(DME)]$ with a CH_2Cl_2 solution of the P,N ligand,^{10,11} similarly to its Co(II) analogue.¹¹ A red powder was obtained by addition of *n*-pentane and single crystals of **14a** formed by slow diffusion of a toluene-pentane mixture into a CH_2Cl_2 solution of the complex at 298 K. No NMR characterization of the complexes described in this work was possible owing to their paramagnetic nature.



In the molecular structure of **14a** (Figure 1), the metal center is chelated by a molecule of the P,N ligand $Ph_2POCH_2C\equiv NCM_e_2CH_2O$ with a bite angle of 90.5(2)°. The chelate ring defined by P1, O2, C6, C5, N1, Ni1 adopts a boat conformation. Two terminal chlorides are also bound to the metal center whose coordination geometry is distorted tetrahedral. The structure is similar to that of the complex $[NiCl_2\{Ph_2POCMe_2ox^{Me_2}\}]$ ($Ph_2POCMe_2ox^{Me_2} = 2-((diphenylphosphinooxy)propan-2-yl)-4,4-$ dimethyl-4,5-dihydrooxazole) **10** which contains a CMe_2 group α to the oxygen (Scheme 1)¹² and to that of the Co(II) complexes $[CoCl_2\{Ph_2POCMe_2ox^{Me_2}\}]$ or $[CoCl_2\{Ph_2POCMe_2ox^{Me_2}\}]$.¹¹ The Ni1–Cl1 distance in **14a** (Ni1–Cl1 2.234(2) Å) is slightly longer than Ni1–Cl2 (Ni1–Cl2 2.179(3) Å), and the Cl2–Ni1–P1 angle (113.9(1)°) is wider than Cl1–Ni1–P1 (101.2(1)°).

(8) (a) Britovsek, G. J. P.; Gibson, V. C.; Wass, D. F. *Angew. Chem., Int. Ed.* **1999**, *38*, 428. (b) Mecking, S. *Angew. Chem., Int. Ed.* **2001**, *40*, 534. (c) Rieger, B.; Saunders Baugh, L.; Kacker, S.; Striegler, S., Eds. *Late Transition Metal Polymerization Catalysis*; Wiley-VCH: Weinheim, 2003. (d) Bianchini, C.; Giambastiani, G.; Guerrero, I. R.; Mantovani, G.; Meli, A.; Segarra, A. M. *Coord. Chem. Rev.* **2006**, *250*, 1391. (e) Bianchini, C.; Gatteschi, D.; Giambastiani, G.; Rios, I. G.; Ienco, A.; Laschi, F.; Mealli, C.; Meli, A.; Sorace, L.; Toti, A.; Vizza, F. *Organometallics* **2007**, *26*, 726. (f) Toti, A.; Giambastiani, G.; Bianchini, C.; Meli, A.; Luconi, L. *Adv. Synth. Catal.* **2008**, *350*, 1855.

(9) Kermagoret, A.; Pattacini, R.; Chavez Vasquez, P.; Rogez, G.; Welter, R.; Braunstein, P. *Angew. Chem., Int. Ed.* **2007**, *46*, 6438.

(10) Agostinho, M.; Braunstein, P.; Welter, R. *Dalton Trans.* **2007**, 759.

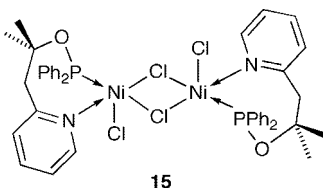
(11) Jie, S.; Agostinho, M.; Kermagoret, A.; Cazin, C. S. J.; Braunstein, P. *Dalton Trans.* **2007**, 4472.

(12) Speiser, F.; Braunstein, P.; Saussine, L.; Welter, R. *Inorg. Chem.* **2004**, *43*, 1649.

Recrystallization of **14a** from a toluene-pentane/ CH_2Cl_2 solution at temperatures below 253 K afforded a mixture of red and green crystals, the latter corresponding to the dinuclear formula isomer complex **14b**. Its proportion increases when the crystallization temperature is lowered to 238 K, where the ratio **14a/14b** is approximately 1:1. An ORTEP plot of the molecular structure of **14b** in $\text{14b} \cdot 2\text{CH}_2\text{Cl}_2 \cdot 2\text{CH}_3\text{C}_6\text{H}_5$ is shown in Figure 2.

Complex **14b** is a chloride-bridged dinuclear compound, similar to the five-membered ring phosphino-oxazoline bromo analog **11**.¹³ The existence of a crystallographic C_2 axis passing through Cl2 and Cl3 results in the planarity of the central Ni_2Cl_2 unit. Each Ni atom is also coordinated by the P,N chelate

$\text{Ph}_2\text{POCH}_2\text{C}=\text{NCMe}_2\text{CH}_2\text{O}$ and by a terminal chloride, giving rise to a distorted square-pyramidal coordination geometry, the base of the pyramid being defined by N1, Cl1, Cl2, and Cl3 and the vertex being occupied by the P1 atom. The distance between Ni1 and the mean plane defined by the basal atoms is 0.330(7) Å. Only four $[(\text{NiCl}_2(\text{P,N}))_2]$ (P, N = chelating ligand) compounds similar to **14b** appear to have been reported in the literature, three of which sharing the same arrangement,^{5,14,15} while in the fourth, the dinuclear phosphinito-pyridine Ni(II) complex **15**, the P atom is in the base of the distorted square-pyramidal structure whose vertex is occupied by a chlorine.¹²



Although the structures of **14a** and **14b** display well-known connectivities, this is the first time, to the best of our knowledge, that the crystal structures of formula isomers of the type $[\text{NiX}_2(\text{P,N})]_n$ (X = Cl, Br; $n = 1, 2$, or 4) have been determined. According to the Cambridge Crystallographic database,¹⁶ there are five different structural types encountered for complexes of the general formula $[\text{NiX}_2(\text{P,N})]_n$ (Scheme 2).⁹

Compound **14a** shows a type II structure, whereas **14b** belongs to the type III family whose structure contains a C_2 symmetry axis. Intuitively, square planar structures (type I) are possible when the steric hindrance in the metal coordination plane is minimized (e.g., when P,N is $\text{Ph}_2\text{PC}(\text{CH}_3)_2$ -*o*-pyridine).^{4c} In **14a** this arrangement would be disfavored because of the presence of the two methyl groups in α position with respect to the nitrogen atom. For similar reasons, the centrosymmetric structures of types IV (e.g., P,N = $\text{Ph}_2\text{POCMe}_2\text{CH}_2$ -*o*-pyridine in **15**)¹² or V (e.g., P,N = Ph_2PCH_2 -2-oxazoline and -thiazoline as in compounds **1** and **3**, respectively, in Scheme 1)⁹ are disfavored with this ligand, being hindered in the position *cis* to the phosphorus atom in the P, Ni, N plane. The P–Ni–N angle can be larger and have more flexibility in a type III vs a type IV structure.⁵ Type V structures require ligands with relatively reduced steric hindrance, both in the chelation plane and toward the axial positions (as with Ph_2PCH_2 -2-thiazoline).

(13) Speiser, F.; Braunstein, P.; Saussine, L.; Welter, R. *Organometallics* **2004**, 23, 2613.

(14) Sun, W.-H.; Li, Z.; Hu, H.; Wu, B.; Yang, H.; Zhu, N.; Leng, X.; Wang, H. *New J. Chem.* **2002**, 26, 1474.

(15) Faissner, R.; Huttner, G.; Kaifer, E.; Kircher, P.; Rutsch, P.; Zsolnai, L. *Eur. J. Inorg. Chem.* **2003**, 2219.

(16) CCDC database November 2007 Update.

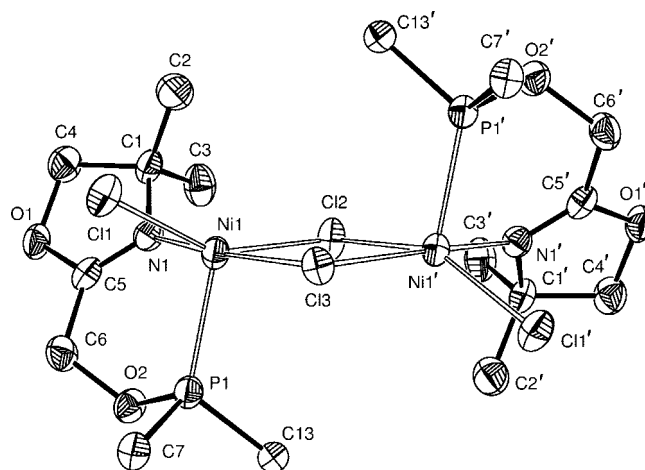


Figure 2. ORTEP plot of the molecular structure of **14b** in $\text{14b} \cdot 2\text{CH}_2\text{Cl}_2 \cdot 2\text{CH}_3\text{C}_6\text{H}_5$. Hydrogen atoms have been omitted and only the phenyl *ipso* carbon atoms are depicted for clarity. Symmetry operations generating equivalent atoms ($'$): $-x, y, -1/2-z$. Selected distances (Å) and angles (deg): Ni1–P1 2.292(1), Ni1–Cl1 2.292(1), Ni1–Cl2 2.334(1), Ni1–Cl3 2.415(1), Ni1–C5 1.265(5); N1–Ni1–Cl1 89.3(1), N1–Ni1–P1 91.2(1), Cl1–Ni1–P1 104.54(5), N1–Ni1–Cl2 89.4(1), Cl1–Ni1–Cl2 151.33(4), P1–Ni1–Cl2 104.12(4), N1–Ni1–Cl3 172.5(1), Cl1–Ni1–Cl3 95.50(4), P1–Ni1–Cl3 93.08(4), Cl2–Ni1–Cl3 83.66(5), Ni1–Cl2–Ni1' 98.54(7), Ni1–Cl3–Ni1' 94.15(6).

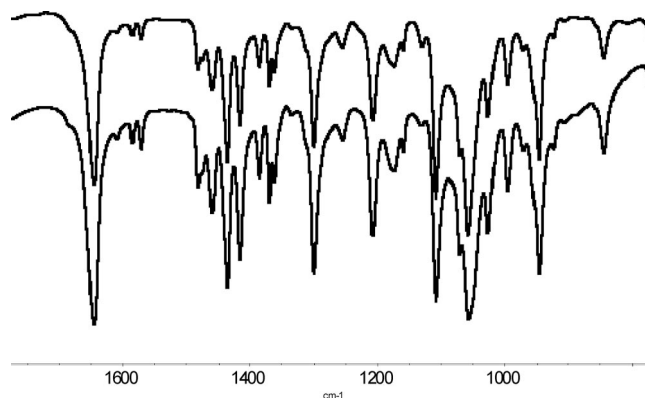
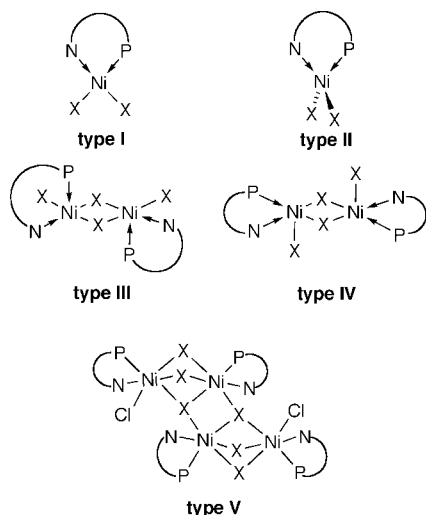


Figure 3. Comparison between the FTIR spectra in the 750–1800 cm^{-1} region of a single crystal of **14a** (upper) and of the product resulting from spontaneous transformation of **14b** above 253 K (lower spectrum).

Green crystals of **14b** obtained at or below 253 K from a toluene-pentane/ CH_2Cl_2 solution turned red in their mother liquor at room temperature. The product of this transformation has been confirmed by FTIR spectroscopy to be **14a**, thus implying that dissociation of the dinuclear complex has occurred in the solid-state. A comparison between the FTIR spectra of a single crystal of **14a** (Figure 3, upper spectrum) and of the red product resulting from the spontaneous transformation of **14b** (Figure 3, lower spectrum) shows that they are superimposable.

The important role played by the crystallization solvent in assisting the solid-state transformation of **14b** to **14a** is noteworthy. The conversion is very slow when the crystals of **14b** are protected by a perfluorinated oil, whereas it is fast when the crystals are exposed to air. In the former case, the crystals become opaque almost immediately, presumably because of rapid loss of the most volatile species in the lattice, CH_2Cl_2 . At this stage, however, no color change occurs. This happens slowly, suggesting that the loss of toluene may be a necessary

Scheme 2



step for the **14b** \rightarrow 2 **14a** fragmentation. This is reminiscent of the pressure-induced isomerization of the tetranuclear complex $[\text{NiCl}_2(\text{Ph}_2\text{PCH}_2\text{-2-oxazoline})]_4$ (type V) in the solid state, which afforded **1** (type I) only after solvent evaporation.⁹ In first approximation, the voids created by the solvent loss facilitate the conversion, as a lattice relaxation (when going from **14b** to **14a**) becomes then possible. A similar solid-state dissociation has been observed with α -diimino complexes of the type $[\text{NiBr}_2[(t\text{-Bu})\text{N}=\text{CHCH}=\text{N}(t\text{-Bu})]]$, however at higher temperature (378 K).¹⁷

In solution, a **14b** \rightleftharpoons 2 **14a** equilibrium is established, since a red dichloromethane/toluene solution becomes green below ca. 220 K, similarly to what was observed with the aforementioned tetramer \rightleftharpoons monomer equilibrium and also observed with other Ni complexes bearing P,N ligands.¹⁸ This is consistent with the proposed equilibrium because of the role played by entropy in dissociation reactions. Binuclear **14b** is thus, qualitatively, enthalpically favored with respect to **14a**. A similar test was performed on red dichloromethane solutions of **6** which bears two exocyclic methyl groups. A color change to green was observed at lower temperatures (ca. 180 K), but no crystal of the corresponding dinuclear species could be grown.

The variable temperature visible/near IR spectra of **14a** (Figure 4) are consistent with the proposed equilibrium. At 298 K the spectrum contains a band at 500 nm in the visible region and a weaker one at 890 nm in the near-infrared. The latter is attenuated at lower temperature, while a new, strong band appears at 440 nm. A shoulder is observed at 500 nm at 173 K, possibly corresponding to the absorption observed at room temperature. A further broad (possibly multiple) absorption appears at 670 nm. This band is not present at 298 K, suggesting that at this temperature the amount of dimer is negligible. The spectrum change is reversible. When the solvent polarity was lowered (by adding Et_2O to the dichloromethane solution), the 440 and 670 nm bands appear at higher temperature, indicating that the dimerization process is favored when the solvent polarity is decreased. It should be mentioned that the band at 440 nm was not observed for the tetranuclear octahedral derivative observed for phosphino-methylthiazoline,⁹ which is consistent with the different nature of the assembled oligomers.

Ethylene Oligomerization Catalyzed by Nickel Complexes Activated with AlEtCl_2 . Table 1 reports the results of a study where the Ni(II) complexes **1–3, 6, 10–12**, and **14a** (40 μmol) were used to catalyze the oligomerization of ethylene in the presence of 2, 4, or 6 equiv of AlEtCl_2 as precatalyst activator.

All these catalytic systems gave almost exclusively butenes and hexenes in ratios increasing with the amount of activator. The selectivity in α -olefins was relatively modest (3–22 mol% estimated on butenes) because of a fast isomerization process, which is typical of Ni(II) oligomerization catalysts.^{6b,c,19} Precatalyst **1** showed the highest activity with TOFs as high as 7.9×10^4 mol C_2H_4 converted $(\text{mol of Ni} \times \text{h})^{-1}$ with 6 equiv of AlEtCl_2 (entry 2), while **14** activated by 2 equiv of AlEtCl_2 gave the lowest ethylene conversion but the most selective system, yielding 96% of C_4 olefins with 22% of 1-butene (entry 14).

Since comparable activities were observed for the bis-chloride **1** and the bis-bromide **2** with either 2 or 6 equiv of AlEtCl_2 , respectively, the halide coligand in the precursor seems to have a negligible influence on the catalytic outcome (Table 1, entries 1 vs 3 and 2 vs 5). Replacing the oxygen atom with sulfur in the oxazoline ring decreased the catalytic activity when only 2 equiv of AlEtCl_2 were used (entry 6 vs entries 1 and 3), but this effect was much less significant in the presence of 6 equiv of this cocatalyst (entry 7 vs entries 2 and 5).

Compared to the catalytic results of the nickel complexes **6, 11** and **12** coordinated by dimethyl-substituted oxazoline moieties,¹³ **1–3** showed higher activities but lower selectivities in butenes (entries 2 vs 13, 2 vs 9, and 5 vs 12).

Ethylene Oligomerization Catalyzed by Nickel Complexes Activated with MAO. Complexes **1–5, 7–9**, and **14** (Scheme 1) have been tested in the ethylene oligomerization using methylaluminoxane (MAO) (2000 equiv) as activator. Table 2 summarizes the results of reactions carried out using 2 μmol of precatalyst in 40 mL of a toluene/chlorobenzene mixture. Under these conditions, no induction period was observed and the maximum activity was attained within a few minutes, then the consumption of ethylene remained practically constant for more than half an hour. All complexes investigated have been found to generate active systems for the production of short-chain olefins, in the $\text{C}_4\text{–C}_{10}$ range, with a Schulz-Flory distribution and turnover frequencies (TOFs) as high as 23×10^4 mol of C_2H_4 converted $(\text{mol of Ni} \times \text{h})^{-1}$ (entry 2). Analogously to what was observed using AlEtCl_2 as activator, the precatalysts featured by the oxazoline system gave the best TOFs, showing similar selectivity in α -olefins. Increasing the ethylene pressure from 4 to 20 bar resulted in an appreciable increase of the selectivity in linear olefins (estimated on the C_6 products, Table 2, entries 4–7), whereas the α factor was independent of the pressure, indicating that both the propagation and chain-transfer rate are first order in ethylene concentration.²⁰ Neither saturated hydrocarbons nor odd carbon oligomers were produced in a detectable amount, which indicates the absence of chain transfer to aluminum.^{20b,21} Conversely, in all oligomerization reactions, mixtures of linear and branched olefins were produced,

(19) (a) Rieger, B.; Baugh, L. S.; Kacker, S.; Striegler, S. *Late Transition Metal Polymerization Catalysis*; Wiley-VCH: Weinheim, 2003; p 331. (b) Johnson, L. K.; Killian, C. M.; Brookhart, M. *J. Am. Chem. Soc.* **1995**, *117*, 6414. (c) Heinicke, J.; Köhler, M.; Peulecke, N.; Kindermann, M. K.; Keim, W.; Köckerling, M. *Organometallics* **2005**, *24*, 344. (d) Yang, Q.-Z.; Kermagoret, A.; Agostinho, M.; Siri, O.; Braunstein, P. *Organometallics* **2006**, *25*, 5518.

(20) (a) Small, B. L.; Brookhart, M. *J. Am. Chem. Soc.* **1998**, *120*, 7143. (b) Britovsek, G. J. P.; Mastroianni, S.; Solan, G. A.; Baugh, S. P. D.; Redshaw, C.; Gibson, V. C.; White, A. J. P.; Williams, D. J.; Elsegood, M. R. *J. Chem. Eur. J.* **2000**, *6*, 2221.

(17) Oswald, H. R.; Beer, H. R. *Mater. Sci. Monogr.* **1985**, *28B*, 893.

(18) Christopher, R. E.; Gordon, I. R.; Venanzi, L. M. *J. Chem. Soc.* **1968**, 205.

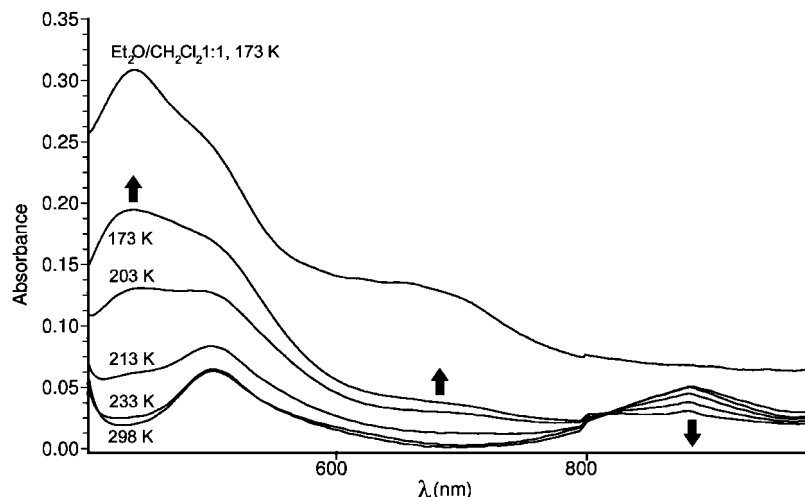


Figure 4. Visible/near IR solution spectra at variable temperature of complex **14a** in the region 400–1000 cm^{-1} . The spectra were recorded in CH_2Cl_2 (4 mM), except the top one, which was recorded in a $\text{CH}_2\text{Cl}_2/\text{Et}_2\text{O}$ 1:1 v/v mixture. For clarity, the top spectrum has been shifted by ca. +0.08 absorbance units.

Table 1. Catalytic Results for Complexes 1–3, 6, 10–12, and 14a in Ethylene Oligomerization using AlEtCl_2 as Activator^a

entry	precatalyst	AlEtCl_2 (equiv)	prod. ^b	$\text{TOF}^c (\times 10^{-4})$	α^d	C_4 g %	C_6 g %	C_8 g %	1-butene mol %
1	1	2	22200	4.65	0.16	80	19	1	9
2	1	6	37650	7.88	0.53	53	42	5	4
3	2	2	21120	4.42	0.25	71	26	3	10
4	2	4	30530	6.39	0.31	68	29	3	4
5	2	6	37170	7.78	0.38	62	34	4	3
6	3	2	5060	1.06	0.11	86	13	1	15
7	3	6	34350	7.19	0.44	58	39	3	4
8	6 ¹³	2	12300	2.54	0.28	67	28	3	25
9	6 ¹³	6	22000	4.59	0.50	54	40	1	20
10	10 ¹²	2	21200	4.44	0.22	81	18	1	14
11	10 ¹²	6	23800	4.99	0.51	64	33	3	8
12	11 ¹³	6	traces	traces		100			
13	12 ¹³	6	18400	3.81	0.34	64	33	3	13
14	14a ^e	2	900	0.19	<0.10	96	3	<1	22
15	14a ^e	4	23220	4.86	0.23	73	25	2	6
16	14a ^e	6	30200	6.32	0.29	69	30	1	7

^a Reaction conditions: stainless steel-reactor, 145 mL; precatalyst: 40 μmol ; solvent: chlorobenzene, 14 or 13 or 12 mL + 1 or 2 or 3 mL of cocatalyst in toluene solution for 2 or 4 or 6 equiv of AlEtCl_2 , respectively; 10 bar of C_2H_4 ; stirring rate: 450 rpm; time 35 min; initial temperature, 25–30 °C. ^b Grams C_2H_4 converted (g of Ni \times h)⁻¹. ^c Mol of C_2H_4 converted (mol of Ni \times h)⁻¹; products quantified by GC (average value over two runs at least). ^d $\alpha = \text{mol of C}_6 / (\text{mol of C}_4)^{-1}$. ^e Presence of **14a** under the catalytic conditions is favored by the increased temperature.

Table 2. Catalytic Results for Complexes 1–5, 7–9, and 14a in Ethylene Oligomerization using MAO as Cocatalyst^a

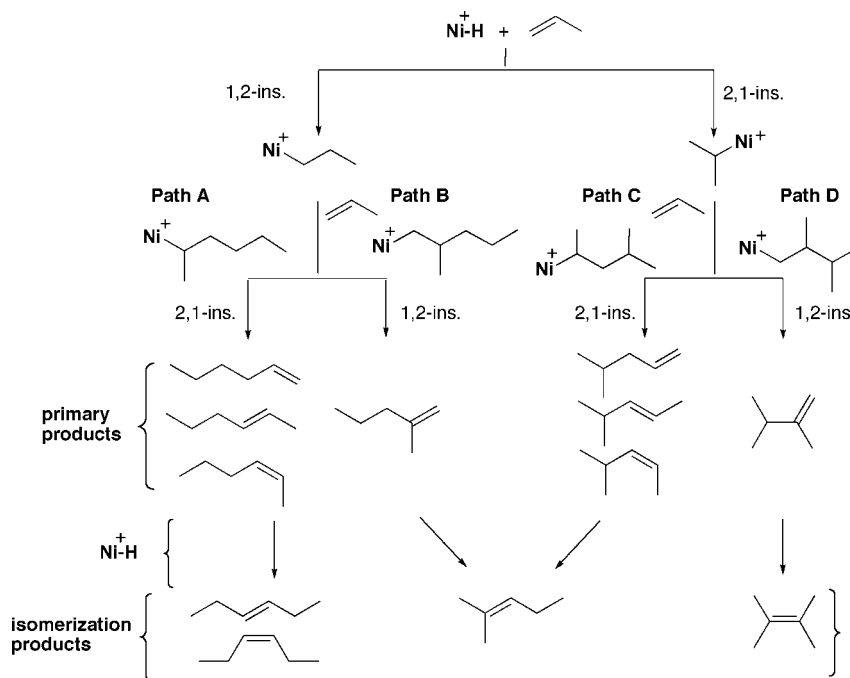
entry	precatalyst	pressure (bar)	$\text{TOF}^b (\times 10^{-4})$	α^c	C_4 g %	C_6 g %	C_8 g %	C_{10} g %	1-hexene mol %	linear C_6 (%) ^d
1	1	10	10.82	0.12	75.3	19.8	4.1	0.7	14.0	79.3
2 ^e	1	10	22.86	0.12	74.3	20.4	4.4	0.8	15.3	75.6
3	2	10	6.44	0.14	69.7	25.6	4.1	0.5	14.8	77.1
4	3	4	1.93	0.07	89.8	9.3	0.8	<0.1	9.6	80.7
5	3	10	5.92	0.07	89.1	10.2	0.6	<0.1	13.8	70
6	3	15	8.61	0.08	83.5	14.3	1.9	0.2	15.1	91.2
7	3	20	14.95	0.07	90.9	8.4	0.6	<0.1	17.3	92.6
8	4	10	5.36	0.11	77.1	18.7	3.6	0.5	15.4	78.8
9	5 ^f	10	2.76	0.13	72.9	21.2	4.9	0.9	12.2	73.4
10	7	10	6.09	0.16	67.9	23.8	6.6	1.4	14.6	80.7
11	8	10	5.33	0.08	81.8	15.5	2.3	0.3	14.6	80.3
12	9	10	3.15	0.11	76.6	19.0	3.7	0.6	11.8	72.5
13	14a ^g	10	6.43	0.11	76.5	19.1	3.7	0.6	16.7	73.6

^a Reaction conditions: stainless steel-reactor, 1 L; precatalyst: 2 μmol ; cocatalyst: MAO, 4 mmol (2000 equiv); toluene, 39 mL + 1 mL of chlorobenzene as cosolvent; stirring rate: 1500 rpm; time 30 min; temperature 30 \pm 1 °C. ^b Mol of C_2H_4 converted (mol of Ni \times h)⁻¹; products quantified by GC using *n*-heptane as internal standard (average value over three runs). ^c Schulz-Flory parameters, $\alpha = \text{mol of C}_{n+2} / (\text{mol of C}_n)^{-1}$. ^d Determined after hydrogenation of the final reaction mixture using 10% Pd/C and 10 bar of H_2 at room temperature. ^e Ten minutes. ^f This complex was prepared in situ. ^g Presence of **14a** under the catalytic conditions is favored by the increased temperature.

as shown by the analysis of the hydrogenated reaction mixtures (see Table 2). A rationale for the observed selectivity may be proposed by assuming that the isomerization rate of the Ni-alkyl intermediate prevails over the associative displacement and the migratory insertion. On the other hand, the concomitant

occurrence of reincorporation of the olefins produced at the early stages of the reactions, although unlikely, cannot be definitively ruled out. Experiments with the most active system **1**/MAO showed the composition of the oligomerization mixture (linear and branched isomers) to be independent of the reaction time

Scheme 3. Propylene Dimerization Pathways and Isomerization of Primary Products

Table 3. Propene Oligomerization with Nickel(II) Catalysts 1–5, 7–9, and 14^a

entry	pre catalyst	product mass (g)	TOF ^b ($\times 10^{-4}$)	C ₆ product distribution (%) ^c								
				C ₆ (%)	C ₉ (%)	pathway A ^d				pathway B ^e /C ^f	pathway D ^d	
						linear dimers	1-hexene and 3-(Z)-hexene	2-(E)-hexene	2-(Z)-hexene	3-(E)-hexene	methyl pentenes ^g	2,3-dimethyl butenes
1	1	3.0	1.42	96.3	3.7	18.4	1.1	10.1	5.9	1.2	76.4	5.2
2	2	3.2	1.52	96.2	3.8	18.4	1.1	10.9	5.1	1.4	76.2	5.3
3	3	2.3	1.10	98.5	1.5	18.2	0.7	11.0	5.3	1.2	71.7	10.1
4	4	2.2	1.04	97.3	2.7	17.7	0.7	10.6	5.2	1.3	71.2	11.1
5	5ⁱ	1.2	0.58	95.0	5.0	23.4	1.8	14.0	5.9	1.8	72.4	4.2
6	7	0.3	0.18	98.3	1.7	13.2	2.1	3.9	7.2	0.1	82.5	4.3
7	8	6.9	3.29	96.7	3.3	13.1	2.1	5.5	6.7	0.8	77.9	7.0
8	9	1.7	0.82	98.7	1.3	21.5	4.0	12.5	5.0	0.0	74.6	3.9
9	14	2.2	1.04	98.6	1.4	17.5	2.2	6.2	8.3	0.9	75.0	7.4

^a Reaction conditions: glass-reactor, 250 mL; precatalyst: 10 μ mol; cocatalyst: MAO, 6 mmol (600 equiv); propylene, 17.5–42.2 g; toluene, 40 mL; stirring rate: 1500 rpm; time 30 min; initial temperature, room temp. ^b Mol of C₃H₆ converted (mol of Ni \times h)⁻¹; average value over three runs. ^c Products quantified by GC using *n*-heptane as internal standard. ^d Propylene 1,2-insertion followed by propylene 2,1-insertion. ^e Propylene 1,2-insertion, followed by propylene 1,2-insertion. ^f Propylene 2,1-insertion, followed by propylene 2,1-insertion. ^g Propylene 2,1-insertion followed by propylene 1,2-insertion. ^h 4-Methyl-pent-1-ene (*E* + *Z*)-4-methyl-pent-2-ene, 2-methyl-pent-1-ene, and 2-methyl-pent-2-ene; total amount determined after hydrogenation of final reaction mixture using 10% Pd/C and 10 bar H₂. ⁱ This complex was prepared *in situ*.

(entries 1 vs 2), which is consistent with a prevalent isomerization path of the Ni-alkyl intermediate.

Finally, it is noteworthy that alkyl substituents on the phosphorus atom have a detrimental effect on the catalytic performance (entries 5 vs 9 and 11 vs 12), while the dibromide precursors are from slightly to moderately less active than their dichloride congeners (entries 1 vs 3 and 5 vs 8).

Propene Dimerization Catalyzed by Nickel Complexes Activated with MAO. On treatment with MAO in toluene, the Ni(II) bishalides P,N complexes **1–5**, **7–9**, and **14** (Scheme 1) were found to generate active and selective systems for the dimerization of propene to internal and branched C₆ products (up to 99%). The total amount of branched isomers was determined after the reaction mixtures were hydrogenated in the presence of an heterogeneous catalyst (10 bar H₂ pressure, Pd/C 10% catalyst). The catalytic results are summarized in Table 3.

Under comparable experimental conditions, precatalyst **8** gave the best TOFs (Table 3, entry 7), while the selectivity in hexenes was similar to that of the other catalysts. Like for the ethylene oligomerization, alkyl substituents at phosphorus decreased the catalytic performance (entries 8 vs 7 and 5 vs 4) while a negligible influence of the nature of the halide coligand was generally observed (entries 2 vs 1 and 4 vs 3).

Discussion

The results obtained in the oligomerization of ethylene clearly show that both AlEtCl₂ and MAO are excellent activators of Ni(II) bis-halides modified with hybrid P,N ligands. Although the different experimental conditions used with either activator do not allow for a reliable comparison of the two catalytic systems, it appears that AlEtCl₂ and MAO generate distinct catalytic systems as shown by the different distribution of the olefins produced (non Schulz-Flory with AlEtCl₂ and Schulz-Flory with MAO).

The mechanism of ethylene oligomerization by Ni(II) complexes supported by the chelating ligands and activated by

(21) (a) Small, B. L.; Brookhart, M.; Bennett, A. M. A. *J. Am. Chem. Soc.* **1998**, *120*, 4049. (b) Chen, Y.; Chen, R.; Qian, C.; Dong, X.; Sun, J. *Organometallics* **2003**, *22*, 4312.

AlEtCl₂ or MAO is well established and does not deserve any comment. Instead it may be worthwhile to comment on the specific steps leading to the formation of various hexene isomers upon propene dimerization on the basis of the structural isomers obtained.²² It is well-known that the isomer distribution depends on several factors, which include the alternative migration of either *n*-propyl or isopropyl groups and the way this migration occurs (either 1,2- or 2,1-), and finally the regioselectivity of the β-H elimination steps when two possibilities exist (Scheme 3, paths A and C). Since linear products and dimethyl butenes account for 17–29% of the total products while methyl-pentenes constitute the major product (up to 83%), some mechanistic conclusions can be drawn from the quantitative analysis of the primary products.

For all catalysts, paths A and D, involving either 2,1- or 1,2-insertion into the *n*-propyl and *iso*-propyl complex, respectively, are less favorable. On the other hand, there is little doubt that paths B and C prevail over paths A and D for propene dimerization, accounting for 77–88% of the C₆ mixture (4-methyl-1-pentene, *cis*-4-methyl-2-pentene, and *trans*-4-methyl-2-pentene and 2-methyl-1-pentene). Unfortunately, the propene insertion selectivity is further complicated by our inability to distinguish by GC the methyl-pentene isomers (2-methyl-1-pentene and *cis,trans*-4-methyl-2-pentene). Indeed, peak overlapping did not allow for a reliable assignment of most favorable insertion path of propene to produce the branched isomers.

Conclusions

We have found in this work that the structure of Ni(II) complexes containing functional P,N-type ligands can experience dramatic changes as a function of relatively minor modifications of the ligand or of the crystallization conditions. This was recently highlighted with the unprecedented interconversion between a mono- and a tetranuclear Ni(II) system.⁹ The complex [NiCl₂{Ph₂POCH₂Ox^{Me₂}}] **14** was isolated in the form of red crystals corresponding to its mononuclear form **14a**, in which the metal center has a distorted tetrahedral coordination geometry, and its recrystallization from a toluene-pentane/CH₂Cl₂ solution at temperatures below 253 K afforded green crystals of the dinuclear, chloride-bridged, formula isomer complex **14b**. Conversion of **14b** to **14a** was observed as a function of temperature, both in the solid-state and in solution. The catalytic performance of Ni(II) phosphino- or phosphinito-oxazoline or phosphino-thiazoline, bishalides in the oligomerization of ethylene and propylene has been evaluated using AlEtCl₂ or MAO as activators. These systems have shown from low to fairly good activity for the oligomerization of ethylene leading almost exclusively to the production of dimers and trimers with relatively modest percentages of α-olefins. The precatalysts containing the oxazoline ligands have shown the highest activity with either activator, but the different distribution of the olefins produced (non Schulz-Flory with AlEtCl₂ and Schulz-Flory with MAO) is consistent with the generation of different catalytic systems. The dimerization of propylene to internal and branched hexenes has been achieved by activation of the precatalysts with MAO. The highest TOF for the dimerization of propylene has been obtained with the pyridine-phosphite Ni(II) complex **8**. One of the currently most active Ni(II) catalyst precursor for propene oligomerization is a dinuclear complex containing a (bis-amido)phosphine ligand,

which in the presence of MAO (Al:Ni ratio = 700), gave TOFs up to $1.2 \times 10^6 \text{ h}^{-1}$.²³

Experimental Part

General Considerations. All air- and/or water-sensitive reactions were performed under nitrogen in flame-dried flasks using standard Schlenk-type techniques. Anhydrous toluene was obtained by means of a MBraun Solvent Purification Systems, while chlorobenzene was obtained by distillation under nitrogen from sodium. Solid MAO for oligomerization was prepared by removing toluene and AlMe₃ under vacuum from a commercially available MAO solution (10 wt% in toluene, Crompton Corp.). The MAO solution was filtered on a D4 funnel and evaporated to dryness at 50 °C under vacuum. The resulting white residue was heated further to 50 °C under vacuum overnight. A stock solution of MAO was prepared by dissolving solid MAO in toluene (100 mg mL⁻¹). The solution was used within three weeks to avoid self-condensation effects of the MAO. AlEtCl₂ as a 1 M solution in hexane was used as provided by the supplier. All the other reagents and solvents were used as purchased from commercial suppliers. Catalytic reactions were performed in a 250 mL glass reactor or 500 or 1000 mL stainless steel reactors, equipped with a magnetic drive stirrer and a Parr 4842 temperature and pressure controller. For ethylene oligomerization, the reactor was connected to an ethylene reservoir to maintain a constant pressure throughout the catalytic runs. IR spectra in the range 4000–650 cm⁻¹ were recorded on a Thermo Nicolet 6700 instrument, equipped with SMART Orbit Diamond ATR accessory. Single crystals FTIR spectra were recorded in a diamond window microcompression cell, on a Thermo Nicolet Centaurus microscope. The variable temperature visible spectra of **14a** were recorded on a VARIAN Cary05E, equipped with a OXFORD INSTRUMENTS DN1704 cryostat. Elemental C, H, N analyses were performed by the “Service de microanalyses”, Université de Strasbourg, on a Flash EA 1112 microanalyzer. GC analyses of the reaction products were performed on a Shimadzu GC-17 gas chromatograph equipped with a flame ionization detector and a Supelco SPB-1 fused silica capillary column (30 m length, 0.25 mm i.d., 0.25 μm film thickness) for the C₄–C₁₂ fraction. In the propene dimerization experiments, the yields of dimers and trimers were determined by comparing the integrals of the products to those of the internal standard (*n*-heptane) and by assuming equal response factors of the standard and the products. Specific GC analyses for the C₆ isomers were performed with a Varian PLOT fused silica capillary column with stationary phase PLOT Al₂O₃/KCl (50 m, 0.32 mm i.d., 5 μm film thickness). The GC/MS analyses were performed on a Shimadzu QP2010S apparatus equipped with a column identical with that used for GC analysis.

Preparation of [Ni{2-((diphenylphosphinoxy)methyl)-4,4-dimethyl-4,5-dihydrooxazole}Cl₂] (14a**).** Solid [NiCl₂(DME)] (3.26 g, 14.8 mmol) was added to a solution of the ligand 2-((diphenylphosphinoxy)methyl)-4,4-dimethyl-4,5-dihydrooxazole (4.64 g, 14.8 mmol)^{10,11} in 100 mL of CH₂Cl₂. The solution became red and was stirred overnight. After reaction, unreacted [NiCl₂(DME)] was eliminated by filtration. The solution was concentrated to 30 and 120 mL of pentane were added to precipitate **14a**. After filtration, **14a** was washed with diethylether, dried under vacuum, and isolated as a red powder. Yield: 4.80 g (10.8 mmol, 73%). IR (KBr) cm⁻¹: 1605 (vs), 1484 (vs), 1437 (vs), 1377 (m), 1158 (m), 1101 (s), 1025 (m), 998 (m), 869 (m), 757 (s sh), 743 (s), 718 (m), 698 (vs), 526 (s), 500 (m), 475 (m). HRMS: exp. 406.0268 (M⁺ – Cl), theor. for [C₁₈H₂₀CINNiO₂P]⁺ 406.0278. Anal. calcd for C₁₈H₂₀NCl₂NiPO₂: C, 48.81; H, 4.55; N, 3.16. Found: C, 48.97; H, 4.80; N, 2.91.

General Procedure for the Ethylene Oligomerization. AlEtCl₂ as Activator. The catalytic reactions were carried out in a magnetically stirred (450 rpm) 145 mL stainless steel autoclave. A 125 mL glass container was used to protect the inner walls of the

(22) Bianchini, C.; Giambastiani, G.; Guerrero Rios, I.; Meli, A.; Segarra, A. M.; Toti, A.; Vizza, F. *J. Mol. Cat. A: Chem.* **2007**, *277*, 40.

autoclave from corrosion; 40 μmol of Ni complex were dissolved in 14, 13, or 12 mL of chlorobenzene depending of the amount of the activator and injected into the reactor under an ethylene flux. Then 1, 2, or 3 mL of AlEtCl_2 in toluene, corresponding to 2, 4, or 6 equiv respectively, were introduced into the reactor to achieve a total volume of 15 mL with the precatalyst solution.

All catalytic tests were started between 25 and 30 $^\circ\text{C}$, and no cooling of the reactor was done during the reaction. After injection of the catalytic solution and of the cocatalyst under a constant low flow of ethylene, the reactor was pressurized to 10 bar. A temperature increase was observed due to the remarkable exothermicity of the reactions. The 10 bar working pressure was maintained during the experiments through a continuous feed of ethylene from a reserve bottle placed on a balance to allow continuous monitoring of the ethylene uptake. At the end of each test (35 min) a dry ice bath, and in the more exothermic cases, also liquid N_2 , was used to rapidly cool down the reactor and quench the reaction. When the inner temperature reached 0 $^\circ\text{C}$ the ice bath was removed allowing the temperature to slowly rise to 10 $^\circ\text{C}$. The gaseous phase was then transferred into a 10 L polyethylene tank filled with water. An aliquot of this gaseous phase was transferred into a Schlenk flask, previously evacuated, for the GC analysis. The products in the reactor were treated in situ by addition of ethanol (1 mL), transferred into a Schlenk flask, and separated from the metal complexes by trap-to-trap evaporation (20 $^\circ\text{C}$, 0.8 mbar) into a second Schlenk flask previously immersed in liquid nitrogen to avoid any loss of product.

MAO as Activator. A 1 L stainless steel reactor was heated to 60 $^\circ\text{C}$ under vacuum overnight and then cooled to room temperature under a nitrogen atmosphere. A MAO solution, prepared by diluting 2.65 mL of a stock toluene solution of MAO (4 mmol) with toluene (36.5 mL), was introduced by suction into the reactor, previously evacuated by a vacuum pump. The system was pressurized with ethylene to 10 bar and stirred for 5 min. Afterward, the ethylene pressure was released slowly and 1 mL of a precatalyst solution, prepared by dissolving the solid precatalyst (20 μmol) in 10 mL of chlorobenzene, was syringed into the reactor. The system was pressurized to the final ethylene pressure and stirred at 1500 rpm. Ethylene was continuously fed to maintain the reactor pressure at the desired value. The temperature inside the reactor increased solely from the exothermicity of the reaction and reached a maximum value within 5–7 min. After 30 min, the reaction was stopped by cooling the reactor to -20 $^\circ\text{C}$, depressurizing, and introducing 2 mL of acidic MeOH (5% HCl). *n*-Heptane was injected into the reactor as the GC internal standard and the reactor contents were stirred for 10 min further. The solution was analyzed by GC and GC-MS. The moles of the C6 and C8 fractions were determined by GC using calibration curves with standard toluene solutions containing concentrations of 1-hexene and 1-octene as close as possible to those in the sample under analysis. Schulz-Flory α constants were determined by the molar ratio of the couple C_8/C_6 .

The moles of C_4 were calculated by the Schulz-Flory α constant and the moles of C_6 by the formula moles of $\text{C}_4 = (\text{moles of } \text{C}_6)/\alpha$, whereas the moles of the higher oligomers were calculated by the Schulz-Flory α constant and the moles of C_8 by the general formula moles of $\text{C}_i = (\text{moles of } \text{C}_8)\alpha^{(i-8)/2}$. The total moles of converted ethylene were obtained by the formula moles of $\text{C}_2\text{H}_4 = \sum(\text{moles of } \text{C}_i)(i/2)$ with $i = 4-14$; therefore, the TOFs were obtained.

Oligomerization of Propene. A 250 mL glass reactor equipped with a mechanical stirrer and an external jacket for the temperature control and previously evacuated by a vacuum pump, was charged by suction with 10 mL of toluene. Afterward, a solution of the precatalyst (10 μmol) prepared by dissolving the solid complex in

Table 4. Selected Data Collection and Refinement Parameters for 14a and 14b \cdot 2CH₂Cl₂ \cdot 2CH₃C₆H₅

compound	14a	14b \cdot 2CH ₂ Cl ₂ \cdot 2CH ₃ C ₆ H ₅
Chemical formula	$\text{C}_{18}\text{H}_{20}\text{Cl}_2\text{NNiO}_2\text{P}$	$\text{C}_{36}\text{H}_{40}\text{Cl}_4\text{N}_2\text{Ni}_2\text{O}_4\text{P}_2 \cdot 2\text{CH}_2\text{Cl}_2 \cdot 2\text{C}_7\text{H}_8$
M_r	442.93	1239.98
Cell setting, space group	Orthorhombic, $Pna2_1$	Monoclinic, $P2/c$
Temperature (K)	173(2)	173(2)
a, b, c (\AA)	17.4440(3), 13.5450(8), 8.459(1)	11.7438(5), 12.3426(9), 22.748(1)
β (deg)	90	118.647 (3)
V (\AA^3)	1998.7 (3)	2893.7 (3)
Z	4	2
D_x (Mg m^{-3})	1.472	1.423
Radiation type	Mo $\text{K}\alpha$	Mo $\text{K}\alpha$
μ (mm^{-1})	1.33	1.12
Crystal size (mm)	$0.05 \times 0.04 \times 0.03$	$0.08 \times 0.03 \times 0.03$
No. of meas., indep. and obsvd. Refl.	12329, 3642, 2660	17643, 6614, 3124
R_{int}	0.081	0.086
θ_{max} ($^\circ$)	25.5	27.5
$R[F^2 > 2s(F^2)]$, $wR(F^2)$, S	0.084, 0.202, 1.18	0.059, 0.149, 1.01
No. of parameters	228	290

1 mL of chlorobenzene was syringed under nitrogen atmosphere. The reactor was then cooled at -15 $^\circ\text{C}$ and liquid propene (17.5–42.2 g) was transferred from a 1.5 L cylinder into the reactor via a flexible hose while the internal pressure raised 4–5 bar. The amount of propene used for each run was determined by measuring the cylinder weight difference before and after the propene addition. MAO (6 mmol, ca. 600 equiv, 4 mL) was injected into the reactor via a syringe and the system was warmed to room temperature and the solution stirred. The reactor internal pressure rapidly reached 10 bar. After the desired reaction time, the reactor was depressurized and the mixture was quenched by introducing acidic MeOH (5% HCl, 1 mL). Finally, the reactor mixture was cooled at 0 $^\circ\text{C}$ and the unreacted propene was carefully evaporated under vigorous stirring. A solution of *n*-heptane (1 mL) was added into the reactor as the GC internal standard and an aliquot of the resulting solution was sampled for the GC analyses of the products.

Hydrogenation of the α -Olefin Oligomerization Products. The hydrogenation of the reaction mixtures was carried out in a 20 mL stainless steel autoclave equipped with a magnetic stirrer at room temperature and 10 bar H_2 pressure for 10 h, using Pd/C 10% (80 mg) as catalyst. The quantification of both linear and branched hydrocarbon species was achieved by GC.

X-Ray Data Collection, Structure Solution, and Refinement for Compounds 14a and 14b \cdot 2CH₂Cl₂ \cdot 2CH₃C₆H₅. Suitable crystals for the X-ray analysis of 14a and 14b \cdot 2CH₂Cl₂ \cdot 2CH₃C₆H₅ were obtained as described above. The intensity data were collected at 173(2) K on a Kappa CCD diffractometer²⁴ (graphite monochromated Mo $\text{K}\alpha$ radiation, $\lambda = 0.71073$ \AA). Crystallographic and experimental details for the structures are summarized in Table 4. The structures were solved by direct methods (SHELXS-97) and refined by full-matrix least-squares procedures (based on F^2 , SHELXL-97)²⁵ with anisotropic thermal parameters for all the non-hydrogen atoms. The hydrogen atoms were introduced into the geometrically calculated positions (SHELXS-97 procedures) and refined riding on the corresponding parent atoms. CCDC 704525 (14a) and 704526 (14b) contain the supplementary crystallographic data for this paper that can be obtained free of charge from the Cambridge Crystallographic Data Centre via www.ccdc.cam.ac.uk/data_request/cif.

(24) Bruker-Nonius *Kappa CCD Reference Manual*, Nonius BV: The Netherlands, 1998.

(25) Sheldrick, G. M. *SHELXL-97, Program for crystal structure refinement*; University of Göttingen: Germany, 1997.

(23) Majoum-Mbe, F.; Lönnecke, P.; Volkis, V.; Sharma, M.; Eisen, M. S.; Hey-Hawkins, E. J. *Organomet. Chem.* **2008**, *693*, 2603.

Acknowledgment. We thank the Centre National de la Recherche Scientifique (CNRS), the Ministère de l'Éducation Nationale et de la Recherche (Paris), the Institut Français du Pétrole (IFP), the European Commission (NoE IDE-CAT, NMP3-CT-2005-011730), and the Ministero dell'Istruzione, dell'Università e della Ricerca of Italy (NANOPACK-FIRB project n. RBNE03R78E) for support. We are

grateful to the COST-D30 programme for a mobility grant to P.C.V. We thank Dr. D. Mandon for assistance with the variable-temperature vis/near IR measurements and M. Mermillon-Fournier (LCC Strasbourg) for technical assistance.

OM8009848